Far-field radiation of photonic crystal organic light-emitting diode

Yong-Jae Lee, Se-Heon Kim, Guk-Hyun Kim, and Yong-Hee Lee

Department of Physics, Korea Advanced Institute of Science and Technology, Daejeon 305-701, Korea
yyjjlee@unitel.co.kr

Sang-Hwan Cho, Young-Woo Song, and Yoon-Chang Kim

Research & Development Center, Samsung SDI Co., Ltd.,Yongin, Kyeonggi, 449-902, Korea

Young Rag Do

Department of Chemistry, Kookmin University, Seoul 136-702, Korea

Abstract: Utilizing the near- to far-field transformation based on the 3-D finite difference time domain (FDTD) method and Fourier transformation, the far-field profile of a photonic crystal organic light emitting diode is studied to understand the viewing angle dependence. The measured far-field profiles agree well with those of the simulation. The enhancement of the extraction efficiency in excess of 60% is observed for the optimized photonic crystal pattern.

OCIS codes: (050.1950) Diffraction gratings; (070.2580) Fourier optics; (230.3670) Light-emitting diodes

References and links

1. M. R. Krames, H. Amano, J. J. Brown, P. L. Heremans, "Introduction to the issue on high-efficiency light-emitting diodes," IEEE J. Sel. Top. Quantum Electron. **8**, 185-188 (2002).
2. T. Tsutsui, E. Aminaka, C. P. Lin, and D.-U. Kim, "Extended molecular design concept of molecular materials for electroluminescence: sublimed-dye films, molecularly doped polymers and polymers with chromophores," Philos. Trans. R. Soc. London A **355**, 801-813 (1997).
3. N. K. Patel, S. J. Cinà, and J. H. Burroughes, "High-efficiency organic light-emitting diodes," IEEE J. Sel. Top. Quantum Electron. **8**, 346-361 (2002).
4. M.-H. Lu and J. C. Sturm, "External coupling efficiency in planar organic light-emitting devices," Appl. Phys. Lett. **78**, 1927-1929 (2001)
5. S. Moller and S. R. Forrest, "Improved light out-coupling in organic light emitting diodes employing ordered microlens arrays," J. Appl. Phys. **91**, 3324-3327 (2002).
6. Y.-J. Lee, S.-H. Kim, J. Huh, G.-H. Kim, Y.-H. Lee, S.-H. Cho, Y. C. Kim, and Y. R. Do, "A high-extraction-efficiency nanopatterned organic light-emitting diode," Appl. Phys. Lett. **82**, 3779-3781 (2003).
7. H. J. Peng, Y. L. Ho, X. J. Yu, and H. S. Kwok, "Enhanced coupling of light from organic light emitting diodes using nanoporous films," J. Appl. Phys. **96**, 1649-1654 (2004).
8. J. J. Wierer, M. R. Krames, J. E. Epler, N. F. Gardner, and M. G. Craford, "InGaN/GaN quantum-well heterostructure light-emitting diodes employing photonic crystal structures," Appl. Phys. Lett. **84**, 3885-3887 (2004).
9. J. Huh, J. Ki Hwang, H. Y. Ryu, and Y. H. Lee, " Nondegenerate monopole mode of single defect two-dimensional triangular photonic band-gap cavity," J. Appl. Phys. **92**, 654-659 (2002).
10. H. Y. Ryu, K. S. Kim, S. H. Kwon, H. G. Park, and Y. H. Lee, "Low-threshold photonic crystal lasers from InGaAsP free-standing slab structures," J. Opt. Soc. Korea, **6**, 57-63 (2002).
11. Y. R. Do, Y. C. Kim, Y. W. Song, and Y. H. Lee, "Enhanced light extraction efficiency from organic light emitting diodes by insertion of a two-dimensional photonic crystal structure," J. Appl. Phys. **96**, 7629-7636 (2004).

#7400 - $15.00 US
Received 9 May 2005; revised 19 July 2005; accepted 19 July 2005

12. S. D. Gedney, "An anisotropic perfectly matched layer-absorbing medium for the truncation of FDTD lattices," IEEE Trans. Antennas Propagat. **44**, 1630-1639 (1996).
13. A. Taflove and S. C. Hagness, *Computational Electrodynamics: the finite-difference time-domain method*, (Artech House, Norwood, MA, 2nd ed., 2000).
14. D. J. Shin, S. H. Kim, J. K. Hwang, H. Y. Ryu, H. G. Park, D. S. Song, and Y. H. Lee, "Far- and near-field investigations on the lasing modes in two dimensional photonic crystal slab lasers," IEEE J. Quantum Electron. **38**, 857-866 (2002).
15. H. Rigneault, F. Lemarchand, and A. Sentenac, "Dipole radiation into grating structures," J. Opt. Soc. Am. A **17**, 1048 (2000).

The organic light-emitting diode (OLED) is considered as a critical component for next-generation displays due to its rather simple fabrication processes and low operational voltage [1]. However, because of the high refractive index of the light-emitting layer ($n \sim 1.8$), only a small fraction (< 20 %) of total light is able to escape from the light-emitting dielectric medium into the air. To improve the extraction efficiency and the practicality of OLED devices, various out-coupling schemes have been suggested [2-5]. Authors reported an increase of extraction efficiency of about 50 % from green OLEDs, by introducing a photonic crystal layer on the glass substrate [6]. Recently many other schemes utilizing nano-patterns have also been successfully implemented [7]. A certain scheme was demonstrated even for short-wavelength LEDs [8].

Additionally, in real deployment of the display devices, the angular dependence of the far field radiation is one of the critical issues that have to be taken into consideration in the design of OLEDs. Although the light-emitting excitons in OLEDs are incoherent and distributed randomly over the light emitting layer, the measured far-field pattern shows signatures of the specific symmetry related to the original photonic crystal pattern inscribed in the OLED. The characteristic symmetry in the far field results in the angular variation of light intensity and color and should be understood physically.

Three-dimensional finite-difference time-domain (3D-FDTD) method is employed for the OLED structure schematically described in Fig. 1. This 3D-FDTD method is widely used to describe optical phenomena observable in complex structures such as photonic crystal lasers [9] or photonic crystal LEDs [10]. Our FDTD computation domains representing the PC-OLED structure are explained in Fig. 1. Here the 2D square lattice photonic crystal layer is sandwiched between glass substrate and the transparent ITO electrode. The 2D PC layer is placed at the SiO_2(n=1.45)/Si_xN_y(n=1.95) interface. The Si_xN_y buffer layer (~200 *nm*) is inserted under the ITO electrode to smoothen the ITO/HTL interface. Note that the index of Si_xN_y is similar to that of the ITO/organic layer and larger than that of SiO_2. Now the high-index layer includes the Si_xN_y layer in addition to the original ITO/organic layer. In this case, the expanded high-index guided modes strongly feel the existence of the large index modulation at the boundary. The critical planarization of the Si_xN_y buffer layer was achieved by chemical mechanical polishing processes. Remember that the electrical characteristics can be severely degraded if the ITO surface is not sufficiently smooth [11]. Limited by the computer memory capacity, the domain size of the FDTD computation was restricted to 7x7x3 μm^3 and perfect mirrors were placed at four sides.

The optical absorption in each layer was also considered together with the refraction in order to increase the accuracy of calculation. Typical perfectly matched layer (PML) boundary conditions [12] were employed. The Maxwell equation is now written as Eq. (1).

$$\varepsilon \frac{\partial \vec{E}}{\partial t} = \nabla \times \vec{H} - \sigma \vec{E} \tag{1}$$

where σ(=$2nk\varepsilon_0\omega$) repesents the conductivity and ω is the angular frequency corresponding to the center wavelength of 530 *nm*.

#7400 - $15.00 US Received 9 May 2005; revised 19 July 2005; accepted 19 July 2005

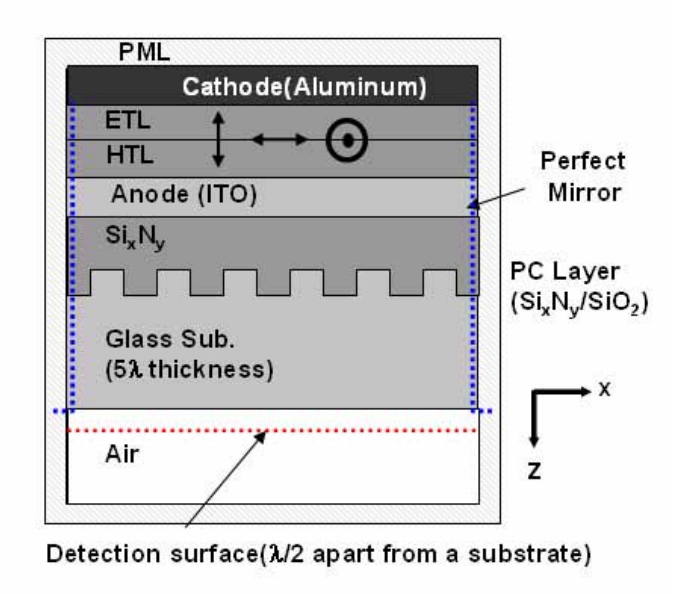

Fig. 1. Schematic of PC-OLED with SiO_2/Si_xN_y photonic crystal layer and computation domain used for the 3-D FDTD method.

In order to model the organic light-emitting diode, the excitons inside the OLED are represented by many Gaussian dipole pulses. Sufficient numbers of horizontal sources (d_x, d_y) and vertical sources (d_z) are distributed randomly over the light-emitting layer. To embody the realistic OLED radiation, sufficiently many *fs*-long dipole pulses are excited randomly over a time span of ~1*ps* in our FDTD computation. The spectrum of this *fs*-long dipole oscillator is centered at a wavelength of 530 nm with full-width-at-half-maximum of 50-nm. Specifically speaking, 1,000 dipoles are fired in every femto-second in the active region between ETL and HTL, for a temporal duration of 1.33*ps*. This corresponds to 40,000 FDTD time steps and the corresponding space resolution is 20 *nm*.

In order to calculate far-field patterns, tangential field components (E_x, E_y, H_x, H_y) derived at the detection surface indicated in Fig. 1 and are stored for each time step. Using this information, the far-field radiation power per unit solid angle $P(\theta, \phi)$ is obtained by Fourier-transforming this near fields into the far fields as follows.[13]

$$P(\theta,\phi) = \frac{\eta}{8\lambda^2}(|N_\theta + \frac{L_\phi}{\eta}|^2 + |N_\phi - \frac{L_\theta}{\eta}|^2) \tag{2}$$

where N_θ, N_ϕ, L_θ, L_ϕ are far fields represented in spherical coordinates,

$$N_\theta = (-FT_2(H_y)\cos\phi + FT_2(H_x)\sin\phi)\cos\theta \tag{3}$$

$$N_\phi = -FT_2(H_y)\sin\phi + FT_2(H_x)\cos\phi \tag{4}$$

$$L_\theta = (FT_2(E_y)\cos\phi - FT_2(E_x)\sin\phi)\cos\theta \tag{5}$$

$$L_\phi = FT_2(E_y)\sin\phi - FT_2(E_x)\cos\phi, \tag{6}$$

#7400 - $15.00 US
Received 9 May 2005; revised 19 July 2005; accepted 19 July 2005

and λ is the center wavelength, η is the characteristic impedance of air, FT_2 represents two-dimensional Fourier transformation. The incoherent far-field pattern can now be obtained by time-integrating the energy flow into each solid angle represented by (θ,ϕ). And from this far-field pattern, one can easily estimate the light extraction efficiency as a function of total viewing angle.

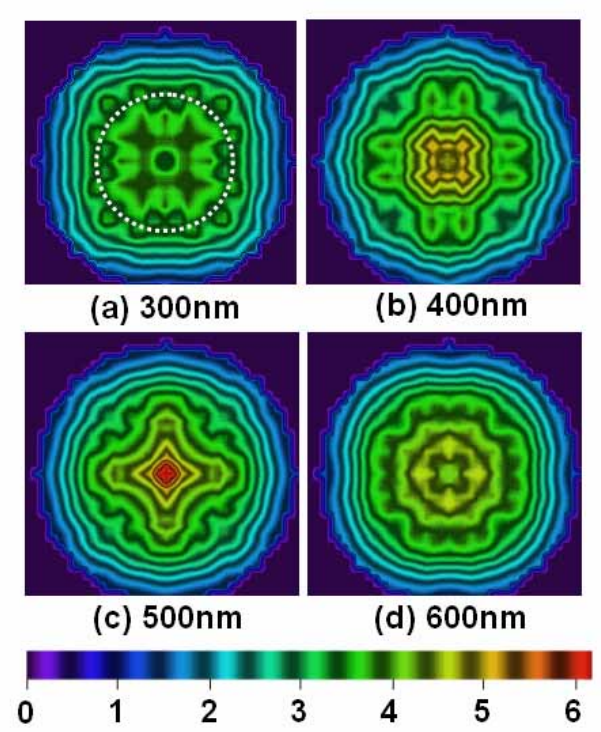

Fig. 2. Calculated far-field profiles for PC-OLEDs of different lattice constants. Dotted circle in (a) represents the viewing cone of angle 45°.

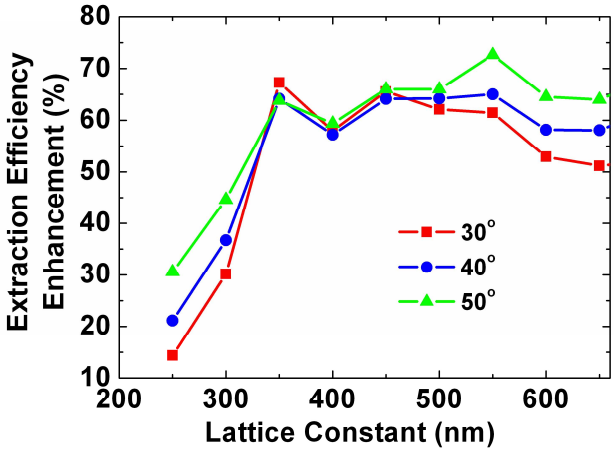

Fig. 3. Relative enhancement of extraction efficiency as a function of lattice constant. Squares – Energy is integrated over viewing angle ±30°. Circles – viewing angle ±40°. Triangles – viewing angle ±50°

#7400 - $15.00 US
Received 9 May 2005; revised 19 July 2005; accepted 19 July 2005

In the design of PC-OLEDs, the important parameters are the lattice constant, the filling factor and the depth of 2-D pattern. Based on our previous experience [11], the rod radius (r) and the pattern depth (d) are chosen as r=0.35Λ and d=350nm, respectively. Here Λ is the period (lattice constant) of the photonic crystal pattern. In fact, this rod radius (r=0.35Λ) had produced the maximum total extraction efficiency and the pattern depth of 350 *nm* is a typical value compatible with holographic lithography. Once these values are fixed, we can focus on the pattern period Λ that gives crucial influence on the far-field profile. For PC-OLEDs of period 300-600 *nm*, computed far-field patterns are plotted following the sphere-to-flat conversion rules [14], as shown in Fig. 2. For short period (300 *nm*) PC-OLEDs, more energy is beamed along the diagonal directions since leaky waves prefer the larger diffraction angle. With increasing Λ (350-550 *nm*), light waves tend to diffract more into shallow angles. In other word, energy flow is concentrated more vertically. But for the larger period of 600 *nm*, the photon energy tends to find the diagonals again because the condition of diffraction is better satisfied at larger angles. For OLED display applications, the angular variation of the extraction efficiency should be considered with care. For example, Fig. 3 shows the relative enhancement of the light extraction as a function of period Λ for three light collection cones of corresponding half angles. It is encouraging to observe the enhancement of the extraction efficiency over 55% for a wide range of period Λ = 350-600 *nm* for viewing angle ±30°.

For comparison purposes, two samples of different periods, Λ=350 nm and 500 *nm*, are prepared. Figure 4 shows fabricated square lattice photonic crystal patterns prepared by two-step holographic lithography. The rod radius of both samples is 0.38Λ. Through FDTD calculation, we found that the PC-OLED of Λ=350 *nm* registers an enhancement of about 67% for viewing angle ±30°. The sample with Λ=500 *nm* shows an enhancement amounting to 76% relative to that of the conventional OLED without a PC pattern.

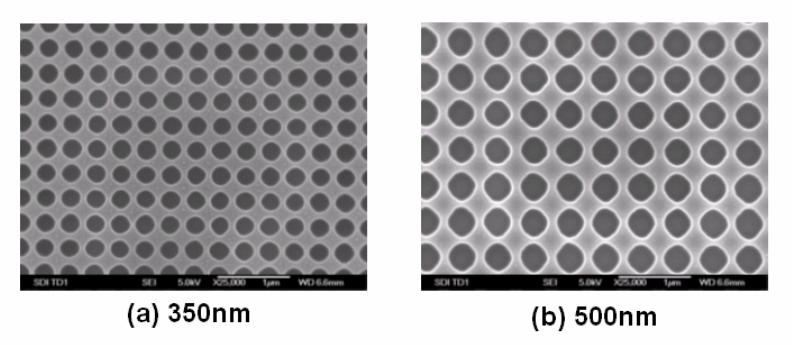

Fig. 4. Scanning electron micrographs of photonic crystal patterns. (a) Lattice constant 350 *nm*. (b) Lattice constant 500 nm. The radius r is ≈ 0.38Λ for both cases.

Using the solid-angle scanner [14], far-field radiation profiles are measured. The experimental far-field profiles in Fig. 5(a) and (b) are taken under the identical current pumping condition. Note that the PC-OLED produces a pattern with four-fold symmetry attributable to the square lattice of the original photonic crystal.[15] For comparison, the calculated far-field profiles are also shown in Fig. 5(d) and (e). In addition, we also measured and calculated the far-field profiles of the thick Si_xN_y-buffer type PC-OLED in Ref [6], as depicted in Fig. 5(c) and (f), respectively. The general agreement between the FDTD calculations and the real data is noticeable, although not perfect. The measured far-field profiles sampled along the horizontal axis are compared with those of the computation in Fig. 6. For the viewing angle ±30°, the fractional increase of the total light extraction is more than

#7400 - $15.00 US Received 9 May 2005; revised 19 July 2005; accepted 19 July 2005

60% for both cases of Λ=350 *nm* and Λ=500 *nm*. The relative deviation between the theory and experiment is less than 7%.

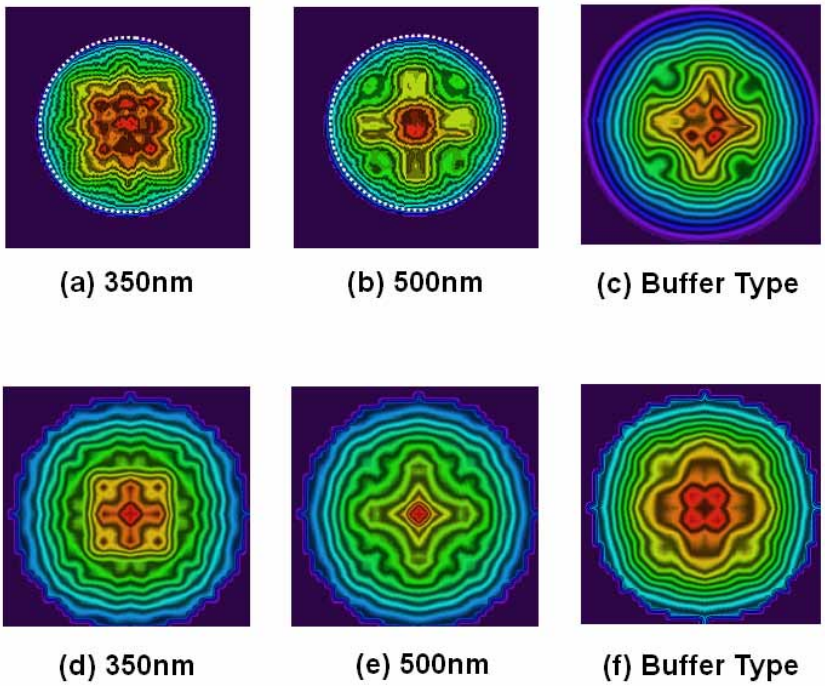

Fig. 5. Measured and calculated far-field profiles. (a) & (b) Solid-angle-scanned profile. The dotted circle represents the angle ±70° from the vertical. (c) Scanned up to the horizon (±90°). (d)-(f) FDTD calculation results. Here the outer-most region corresponds to the horizon.

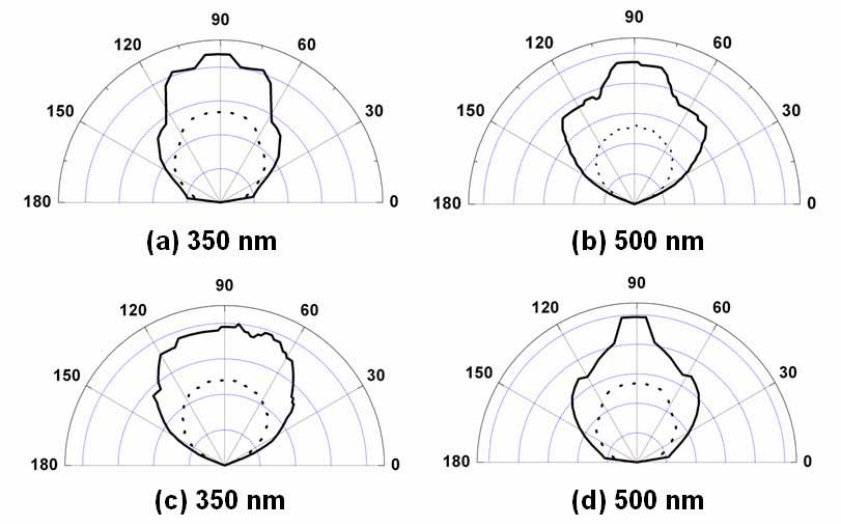

Fig. 6. Intensity profiles scanned along horizontally. (a) and (b) are measured data. (c) and (d) are FDTD calculated profiles. Solid lines are for PC-OLEDs and the dotted line is shown as a reference corresponding to a typical conventional OLED.

#7400 - $15.00 US Received 9 May 2005; revised 19 July 2005; accepted 19 July 2005

In summary, combining the 3-D FDTD method and Fourier transformation, a reliable computational scheme that can deliver the angular profile of the far field of PC-OLEDs is developed. Measured far-field profiles agree reasonably with those obtained from the computation. From the PC-OLED fabricated by the optimized photonic crystal pattern, an increase of the extraction efficiency in excess of 60% was achieved experimentally and the FDTD calculation explains this result faithfully.

Acknowledgement

This work was supported by the Electronic Materials development team of Samsung SDI, Co. Ltd.

#7400 - $15.00 US Received 9 May 2005; revised 19 July 2005; accepted 19 July 2005